Available online at www.sciencedirect.com

ScienceDirect

IFAC PapersOnLine CONFERENCE PAPER ARCHIVE

IFAC PapersOnLine 56-3 (2023) 289–294

Design of Parallel Exoskeleton System for Wrist Tremor Suppression

Sudarsana Jayandan Janakaraj * **Oumar Barry** **

* *Virginia Polytechnic Institute and State University, Blacksburg, VA 24061 USA (e-mail: sudarsanajayandj@vt.edu)*

** *Virginia Polytechnic Institute and State University, Blacksburg, VA 24061 USA (e-mail: obarry@vt.edu)*

Abstract: This paper introduces the design of a Parallel Exoskeleton for Wrist Tremor Suppression (PEWTS). The design features dual six degree-of-freedom (DOF) subsystems that aim to be compact and suppress tremors in both radial/ulnar deviation (RUD) and flexion/extension (FE) motions of the wrist. A linear Series Elastic Actuator is employed, to provide compactness and back drivability to the system which would make the orthoses more human-compatible. The presented study focuses on providing a fundamental understanding of the working of PEWTS and investigating its feasibility through kinematic workspace analysis.

Keywords: Assistive and Rehabilitation Robotics; Healthcare systems

1. INTRODUCTION

Tremors are defined as involuntary and rhythmic oscillations of a body part. Pathological tremors, caused by neurological disorders, most commonly manifest in two forms, Essential tremors (ET) (Louis (2001); Benito-Leon and Louis (2006)) and Parkinson's disease (PD) (Jankovic (2008); Kalia and Lang (2015)). ET are prominently kinetic tremors, that is, felt more during motion of the body part while PD is felt more during idle. Tremors generally are not inherently dangerous but can cause significant discomfort and disability during everyday life (Jeffrey and Binit (2014)). But since the majority of the population affected by pathological tremors are elderly, the reduced accuracy and stability due to tremors might lead to serious injuries (Kaelin-Lang et al. (2011)). This has prompted researchers to explore various methods to address this.

Over the years there have been numerous studies on the stimulation means of suppressing tremors. These stimulative methods such as electrical stimulation (Maneski et al. (2011); Heo et al. (2018); Javidan et al. (1992)) and deep brain stimulation (Lyons and Pahwa (2004)) prove to have high efficiency in suppressing tremors upon first usage. However, they might lead to significant side effects, such as a reduction in efficiency over time or the patient might be clinically contraindicated to these interventions (Pascual-Valdunciel et al. (2021)). Over the pharmacological and interventional techniques, rehabilitation devices have also been researched to alleviate the tremors externally (Pons (2008); Fromme et al. (2019)). These tremor suppression devices can be classified into active, semi-active, and passive (Fromme et al. (2019)). Active suppression devices counteract the tremors by generating a desirably equal and opposite force. Whereas, semi-active and passive orthoses utilize energy dissipation in various amounts to suppress tremors. While passive orthoses might dampen the tremors, they might also offer a resistive force for the voluntary motions of the user unlike in the case of active orthoses (Fromme et al. (2019)). Passive devices generally are lighter in weight compared to active devices but are not tuneable to the user's or the environment's needs. Due to these disadvantages, active orthoses are more prevalent and offer better efficacy (Fromme et al. (2019)).

Contemporary wrist orthoses (Rocon et al. (2020); Taheri (2013); Wang (2022)) have successfully alleviated tremors by applying appropriate forces to the wrist joint. But a majority of them are considered bulky, heavy, almost adding 20% of the arm weight, and non-adaptive to humans which can cause rejection by the user (Fromme et al. (2019)). This brings forth a need for a compact and lightweight design. Parallel exoskeletons, since being spread out along the length of the forearm can prove to be relatively compact. But parallel exoskeleton systems that use fluids for actuation like hydraulic or pneumatic (Taheri (2013)) may require additional components such as valves and pumps that might not be ideal.

This paper presents the design of a parallel exoskeleton system that is aimed to be compact and suppress tremors in both RUD and FE motions without hindering the natural human wrist motion. Since the design is mainly focused on the forearm above the elbow it theoretically does not affect the Supination/Pronation (SUP) motion. The usage of Series Elastic linear actuators (Sensinger and Ff. Weir (2006); Knabe et al. (2014)) will provide the device with compactness and back-drivability which would be favorable for human usage. The paper presents the design of a Parallel Exoskeleton for Wrist Tremor Suppression (PEWTS) in Section 2. Modeling of the kinematics and Dynamics of PEWTS is carried out in Section 3. Finally, the Kinematic Workspace Analysis is investigated in Section 4.

10.1016/j.ifacol.2023.12.039

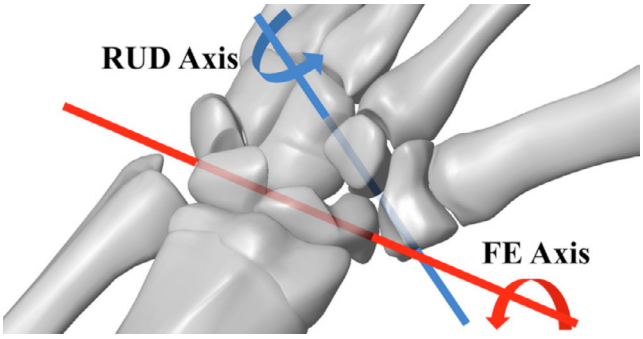

Fig. 1. Approximate position of the rotation axes on wrist (Wang et al. (2020); Moore et al. (2007b))

2. DESIGN OF THE PARALLEL EXOSKELETON FOR WRIST TREMOR SUPPRESSION

To be able to suppress the tremors in the human wrist we should be able to control the two degrees of freedom (DOF) of the wrist, namely the flexion/extension (FE) and radial/ulnar deviation (RUD). While the motion of the wrist can be described with two DOF, the actual kinematics of the wrist is quite complicated. The wrist cannot be accurately modeled as a simple universal joint since there exists an offset between the axes of the two DOF. This is due to the complicated bone structure of the wrist (Moore et al. (2007a)). The approximate relative position of the rotation axes is depicted in Figure 1. This complicated bone structure also results in a coupled translational motion (Li et al. (2005)). Taking into consideration these factors, the wrist joint will be modeled as an ellipsoidal joint model proposed in Wang et al. (2020) to achieve a more realistic model. The wrist is modeled with first-RUD-then-FE rotation sequence.

Since the kinematics of the user's wrist is unknown, the hand and forearm are treated as two separate bodies in 3D space. Hence we need at least 6 DOF to fully control the wrist motion. In conformance with this realization, the Exoskeleton system shown in Figure 2 features two parallel kinematic linkages which are each actuated by a linear actuator. Each subsystem of linkages has 6 DOFs. Thus the linkages have 12 DOFs in total when bases are constrained. Attachments of the exoskeleton onto the arm such as gloves and sleeves have not been depicted in the image. The different poses of the PEWTS covering the circumduction are illustrated in Figure 3. With the current dimensions of the exoskeleton, it can allow the wrist to move from -53deg to 53deg in FE (Flexion-Extension) and -38deg to 32deg in (Radial-Ulnar deviation).

3. MODELING OF PEWTS

To study the feasibility of a system, the design and its 3D motions are not sufficient. Modeling of the said system is required to investigate and quantify the feasibility.

3.1 Kinematic Model of PEWTS

The kinematics of the PEWTS can be studied with the coordinate frames of the subsystem shown in Figure 4. When PEWTS is attached to the arm, the total system

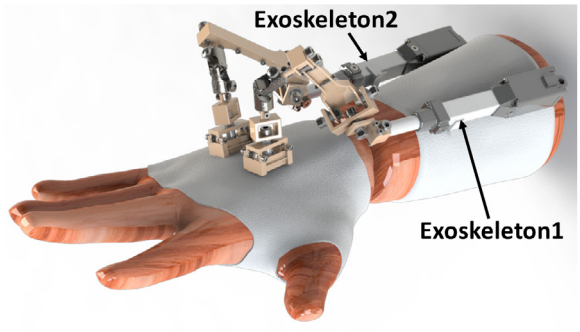

Fig. 2. PEWTS attached to a right forearm mannequin

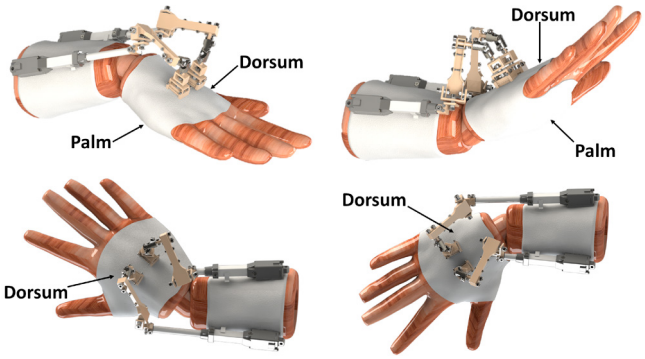

Fig. 3. Different poses of PEWTS installed on right forearm depicting the amount of circumduction covered.

contains three subsystems, the arm subsystem (forearm-wrist-hand) and two exoskeleton subsystems. We investigate the kinematic transformation for one exoskeleton subsystem since the formulations for both subsystems are identical. All the homogeneous transformations are performed with respect to the Grd frame. CG and WG are Common Ground on the forearm and Wrist Ground on the hand, which act as reference frames on the arm subsystem. Physically these frames are the locations where a pair of IMUs (Inertial Measurement Units) [IMU 1 on CG and IMU 2 on WG] will be placed on the user. The IMUs are expected to calculate the orientation of the forearm and hand with respect to the Grd. The transformation between frames $W1$ and $W2$ is the rotation of the wrist. Frames $E1$ and $E2$ are the frames of attachment on the exoskeleton to the forearm and hand respectively. Similarly frames $A1$ and $A2$ are the frames of attachment in the arm subsystem. The frames marked with F are the coordinate frames of the joints of the exoskeleton subsystem.

The three subsystems are modeled as a floating base system, which allows us to input base actuation and excitation. The coordinates of the floating bases are defined in first-order time-derivative form as,

$$\dot{q}_{a,base} = \begin{bmatrix}\dot{\rho}_a^T & \omega_a^T\end{bmatrix}^T ; \dot{q}_{exo_1,base} = \begin{bmatrix}\dot{\rho}_{e1}^T & \omega_{e1}^T\end{bmatrix}^T ; \quad \dot{q}_{exo_2,base} = \begin{bmatrix}\dot{\rho}_{e2}^T & \omega_{e2}^T\end{bmatrix}^T \tag{1}$$

where, $q_{a,base}, q_{exo_1,base}, q_{exo_2,base} \in \mathbb{R}^6$ denotes the base coordinates of the arm subsystem and the two exoskeleton subsystems respectively. The parameters $\rho \in \mathbb{R}^3$ and $\omega \in \mathbb{R}^3$ denote the translational displacements and the angular

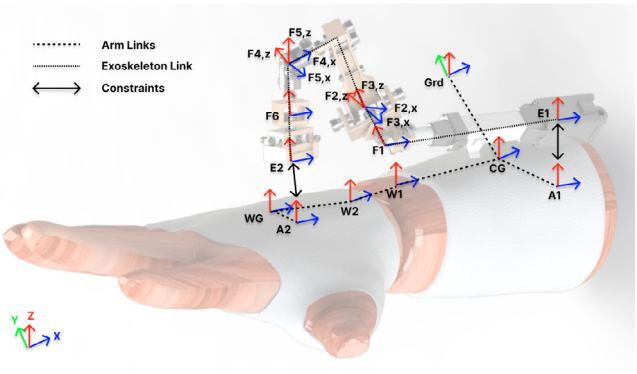

Fig. 4. Coordinate frames of one Exoskeleton subsystem on the left arm (from user's point of view)

velocity with respect to the reference frame. With regard to the orientation, henceforth we shall denote it with $\xi \in \mathbb{R}^4$. Where ξ represents quaternion spatial rotation. We use quaternions in place of Euler angles to avoid the gimbal lock effect (Diebel (2006)) which would ensure a more stable model.

To perform the kinematic transformation on PEWTS we introduce the general homogeneous transformation. The general homogeneous transformation from frame i to j is given by,

$$T_{ij} = \begin{bmatrix} R & d \\ 0_{1\times 3} & 1 \end{bmatrix} = T_{ji}^{-1} \tag{2}$$

where $R \in \mathbb{R}^{3\times 3}$ and $d \in \mathbb{R}^{3\times 1}$ are the rotation matrix and translational displacement associated with the transformation. The homogeneous transformations' properties between the frames for one of the exoskeleton subsystems are specified in Table 1. From the table 1, the quantities, $d_{k,i}$ and $R_k(\theta_i)$ represent the translational displacement and rotational motion along the k axis for i^{th} transformation. When the reference axis of motion k is not specified it is assumed that transformation is with respect to all three axes. The quantities marked by $*$ denote the generalized coordinates of the exoskeleton subsystem. That is

$$q_{exo} = [d_1^* \ \theta_2^* \ \theta_3^* \ \theta_4^* \ \theta_5^* \ \theta_6^*]^T \tag{3}$$

And the generalized coordinates of the wrist subsystem are given as,

$$q_{wrist} = [\theta_{a,1} \ \theta_{a,2} \ \theta_{a,3}]^T \tag{4}$$

where $\theta_{a,1}$, $\theta_{a,2}$ and $\theta_{a,3}$ are the RUD and FE wrist angles and supination (SUP) joint angles respectively.

The properties $\rho_{a,1}|\xi_{a,1}$ $\rho_{a,2}|\xi_{a,2}$, from Table 1, can be obtained from IMU 1, and the difference in spatial properties of IMU 1 and IMU 2 respectively. The transformation between CG and WG, that is from the forearm to the hand, can be performed in two ways, through the exoskeleton subsystem, and from the arm subsystem. When the frames $A_1|E_1$ and $A_2|E_2$ are fully constrained both methods of transformation should be equal. This can be formulated as,

Table 1. Homogeneous transformations' properties between coordinate frames of each exoskeleton subsystem

From	To	Translation (d)	Rotational (R)
G	CG	$d_{a,1} = \rho_{a,1}$	$R(\xi_{a,1})$
CG	E_1	d_{CG}	R_{CG}
E_1	F_1	$d_{x,1} = d^*$	$R_x(\phi)$
F_1	F_2	$d_{z,2}$	$R_z(\theta_2^*)$
F_2	F_3	0	$R_y(\theta_3^*)$
F_3	F_4	d_4	$R_z(\theta_4^*)$
F_4	F_5	0	$R_x(\theta_5^*)$
F_5	F_6	$d_{y,6}$	$R_z(\theta_6^*)$
F_6	E_2	$d_{z,7}$	I
E_2	WG	d_{WG}	I
CG	WG	$d_{a,2} = \rho_{a,2}$	$R(\xi_{a,2})$

$$T_{CG,WG} = \begin{bmatrix} R(\xi_{a,2}) & \rho_{a,2} \\ 0_{1\times 3} & 1 \end{bmatrix} = T_{CG,E_1} \times T_{E_1,E_2} \times T_{E_2,WG} \tag{5}$$

3.2 Nonholonomic Kinematic Constraints

Based on the introduced kinematic model the generalized coordinate system of the forearm-wrist-hand subsystem (arm subsystem) and the two exoskeleton subsystems can be written as,

$$q_a = \left[q_{a,base}^T \ q_{wrist}^T\right]^T ; q_e = \left[q_{e,1} \ q_{e,2}\right]^T \tag{6}$$

$$q_{e,1} = \left[q_{exo_1,base}^T \ q_{exo_1}^T\right]^T ; q_{e,2} = \left[q_{exo_2,base}^T \ q_{exo_2}^T\right]^T$$

This leaves us with a system of 33 DOFs. With proper constraints, the DOF of the system can be reduced. When the floating bases $A_1|E_1$ and $A_2|E_2$ are constrained it restricts 12 DOF on each exoskeleton subsystem. Let us label the constraint on frames $A_1|E_1$ as the base constraint and that on $A_2|E_2$ as the end constraint. The base constraint, $r_{\lambda,base} \in \mathbb{R}^{12}$ can be defined with simple transformation matrices and equality conditions as,

$$r_{\lambda,base} = \begin{bmatrix} q_{a_1,base} = q_{exo_1,base} \\ q_{a_2,base} = q_{exo_2,base} \end{bmatrix} \tag{7}$$

But for the end constraint, a similar approach cannot be performed due to the complexity and the non-holonomic nature of the connection. Thus the end constraint $r_{\lambda,end} \in \mathbb{R}^{12}$ can be written as,

$$r_{\lambda,end} = \left[r_{end,1} \ r_{end,2}\right]^T \tag{8}$$

$$r_{end,1} = \begin{bmatrix} d_{a,end} - d_{e_1,end} \\ [0_{3\times 1} \ I_3]\left(\xi_{a,end}^* \times \xi_{e_1,end}\right) \end{bmatrix}$$

$$\mathrm{r}_{end,2} = \begin{bmatrix} d_{a,end} - d_{e_2,end} \\ [0_{3\times 1} \ I_3]\left(\xi_{a,end}^* \times \xi_{e_2,end}\right) \end{bmatrix}$$

where, $d_{x,end} \in \mathbb{R}^3$ and $\xi_{x,end} \in \mathbb{R}^4$ denote the Cartesian coordinates of the origin and orientation of the end frame in quaternion representation of x subsystem. And ξ^* represents the conjugate of the quaternion. The conjugate of a quaternion has the physical effect of reversing the axis of rotation (Diebel (2006)), therefore by quaternion multiplying the conjugate of the orientation of the attachment frame in the arm to the orientation of the attachment

frame in the exoskeleton the difference in the orientation between the frames can be obtained. If both the frames are aligned then the result of this multiplication will be identity quaternion, $[1, 0, 0, 0]$, when the orientation is unit quaternions.

With the axis-angle representation of a quaternion, defined as $\xi = w + x\hat{i} + y\hat{j} + z\hat{k}$, the orientation can be evaluated. When the rotation is being performed about vector $x_1\hat{i} + y_1\hat{j} + z_1\hat{k}$ with angle ϕ the quaternion is defined as (Diebel (2006)),

$$\begin{aligned} w &= \cos\frac{\phi}{2} \\ x &= x_1 \sin\frac{\phi}{2} \\ y &= y_1 \sin\frac{\phi}{2} \\ z &= z_1 \sin\frac{\phi}{2} \end{aligned} \tag{9}$$

By observing the axis-angle representation of the quaternion (9) it is evident that the vector part of the quaternion, $\left[x\hat{i} + y\hat{j} + z\hat{k}\right]$, contains information about both the axis and the angle. Therefore by multiplying the product of quaternions with $[0_{3\times1}\ I_3]$, in (8), we obtain the optimized information about the difference in orientations of the two frames.

Constraining the supination joint angle is important for stable modeling. When the wrist rotation, between frames $W1$ and $W2$ is ξ_{wrist}, the constraint for SUP angle can be written as,

$$r_{\lambda,wrist} = [1\ 0_{1\times3}]\left([0\ 1\ 0_{1\times2}]^T \xi_{wrist}\right) = 0 \tag{10}$$

Therefore, the total constraints on the system $r_\lambda \in \mathbb{R}^{13}$ is augmented as,

$$r_\lambda = [r_{\lambda,end}\ r_{\lambda,wrist}]^T \tag{11}$$

The first order time derivative of the constraint r_λ from (11) is written as,

$$\dot{r}_\lambda = J_{\lambda,indep}\dot{q}_{indep} + J_{\lambda,dep}\dot{q}_{dep} \tag{12}$$

where, $q_{indep} \in \mathbb{R}^2$ and $q_{dep} \in \mathbb{R}^{13}$ are the independent and dependent generalized coordinates of the whole system, defined as,

$$q_{indep} = [\theta_{a,1}\ \theta_{a,2}]\,; q_{dep} = [\theta_{a,3}\ q_{exo_1}\ q_{exo_2}] \tag{13}$$

And the Jacobian matrices, $J_{\lambda,indep} \in \mathbb{R}^{13\times2}$ and $J_{\lambda,dep} \in \mathbb{R}^{13\times13}$ are the respective Jacobian matrices for the independent and dependent generalized coordinates. Due to the nature of constraints, the first-order time derivative of the constraint equation (12) is equated to zero. If $J_{\lambda,dep}$ is a full rank matrix then the first order time derivative of the dependent generalized coordinate in terms of independent coordinate can be written as,

$$\dot{q}_{dep} = -J^{-1}_{\lambda,dep} J_{\lambda,indep}\dot{q}_{indep} \tag{14}$$

The acceleration of the dependent generalized coordinate can be obtained by further differentiating (14) with respect to time as,

$$\begin{aligned} \ddot{q}_{dep} = -J^{-1}_{\lambda,dep}\,(& J_{\lambda,indep}\ddot{q}_{indep} + \dot{J}_{\lambda,indep}\dot{q}_{indep} \\ & -\dot{J}_{\lambda,dep}J^{-1}_{\lambda,dep}J_{\lambda,indep}\dot{q}_{indep}\Big) \end{aligned} \tag{15}$$

This shows that if the Jacobian matrix $J_{\lambda,dep}$ is full rank then it is possible to related derivatives of q_{dep} with q_{indep}, essentially reducing the DOF of the system to 2 when fully constrained.

3.3 Dynamical Model of PEWTS

With the introduced Kinematic model the dynamics of each subsystem can be derived. When fully unconstrained the equation of motion of the arm subsystem and the exoskeleton subsystem can be written as,

$$\begin{aligned} M_a(q_a)\,\ddot{q}_a = {} & C_a(t, q_a, \dot{q}_a) \\ & + J^T_{u,a}(q_a)\,u_a + J^T_{\lambda,a} + J^T_{w,a}(q_a)\,w_a \end{aligned} \tag{16}$$

$$\begin{aligned} M_e(q_e)\,\ddot{q}_e = {} & C_e(t, q_e, \dot{q}_e) \\ & + J^T_{u,e}(q_e)\,u_e + J^T_{\lambda,e} \end{aligned} \tag{17}$$

where, $q_a \in \mathbb{R}^9$ and $q_e \in \mathbb{R}^{24}$ defines the generalized coordinates of the floating base arm subsystem and the exoskeleton subsystem respectively; $u_a \in \mathbb{R}^9$ defines the human muscle input acting on the floating base and wrist with the assumption that the input is forces and torques and $u_e \in \mathbb{R}^2$ defined the exoskeleton inputs; $w_a \in \mathbb{R}^9$ accounts for disturbance in the arm subsystem and it's assumed that there are no disturbances in the exoskeleton subsystem; $M_a \in \mathbb{R}^{9\times9}$ and $M_e \in \mathbb{R}^{24\times24}$ are the respective generalized mass-inertia matrix; $C_a \in \mathbb{R}^9$ and $C_e \in \mathbb{R}^{24}$ are the combined internal forces consisting of Coriolis term, centripetal, potential and damping forces, and gravitation forces. The matrices $J_{u,a} \in \mathbb{R}^{9\times9}$ and $J_{u,e} \in \mathbb{R}^{2\times24}$ are jacobian matrices of respective inputs, while $J_{w,a} \in \mathbb{R}^{9\times9}$ is the jacobian matrix of disturbance in arm subsystem.

4. KINEMATIC WORKSPACE ANALYSIS

A kinematic workspace analysis is essential to quantitatively determine the feasibility of the system. From Figure 3, the extremes of the circumduction covered by the exoskeleton system are shown, but a workspace analysis is required to determine if the actuators can provide the required inputs comfortably to achieve this circumduction.

4.1 Coupled Dynamics Model and Feasibility Formulation

To perform the Kinematic Workspace Analysis, coupling of the subsystems is required. Constraining the bases of the subsystem with the constraint from (7), the coupled dynamics equation is given by,

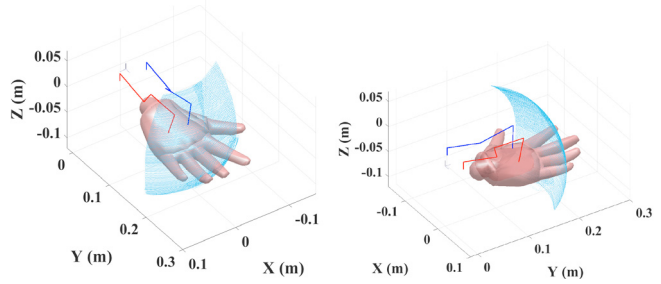

Fig. 5. 3D Visualization of reachability of a PEWTS equipped wrist's motion

$$M_{cp}\left(q_{cp},\zeta_{cp}\right)\ddot{q}_{cp} = -C_{cp}\left(q_{cp},\ddot{q}_{cp},\zeta_{cp}\right)\dot{q}_{cp} + J_{u,cp}^{T}\left(q_{cp},\zeta_{cp}\right)u_{cp} + J_{w,cp}^{T}\left(q_{cp},\zeta_{cp}\right)w_{cp} \tag{18}$$

$$\dot{\zeta}_{cp} = J_{\zeta,cp}\left(q_{cp},\zeta_{cp}\right)\dot{q}_{cp} \tag{19}$$

where ζ_{cp} denotes the nonholonomic states of the system that cannot be written in terms of the generalized coordinates in closed form. With the base constrain in place (7), $q_{cp} \in \mathbb{R}^2$ and $\zeta_{cp} \in \mathbb{R}^{13}$ essentially become q_{indep} and q_{dep} from (13) and $J_{\zeta,cp}$ is the jacobian matrix relating these two coordinates from (14). That is,

$$J_{\zeta,cp} = -J_{\lambda,dep}^{-1}J_{\lambda,indep} \tag{20}$$

Wang (2022) defines the control-targeting dynamical model as,

$$M_{ct}\ddot{q}_{ct} = -C_{ct}\dot{q}_{ct} - g_{ct} + J_{u,ct}^{T}u_{ct} + J_{w,ct}^{T}w_{ct} \tag{21}$$

where the jacobian matrix $J_{u,ct}$ determines the controllability of the system. This input Jacobian matrix for controllability is defined as,

$$J_{u,ct} = \left[I_2 \;\; J_{\zeta,cp}\right]^T \tag{22}$$

Using this input jacobian matrix for controllability, the input jacobian matrix from the exoskeleton subsystem can be obtained by,

$$J_{u,exo} = J_{u,e}J_{u,ct} \tag{23}$$

where $J_{u,e}$ is the jacobian matrix from (17). With $J_{u,exo} \in \mathbb{R}^{2\times2}$ we can determine the feasibility of the exoskeleton in the workspace. Since $J_{u,exo}$ directly relates the actuator input to wrist motion, we can relate the feasibility of input with the wrist position.

If absolute values of the eigenvalues of $J_{u,exo}$ are large enough then the actuators can comfortably perform the required inputs for the specific wrist angle. This factor can be quantified by taking the ratio of the eigenvalues of $J_{u,exo}$. This eigenvalue's norm ratio is given by,

$$n = \frac{z_{u,exo,min}}{z_{u,exo,max}} \tag{24}$$

where, $z_{u,exo,min}$ and $z_{u,exo,max}$ are the minimum and maximum of the absolute eigenvalues of $J_{u,exo}$ respectively. n being close to 1 would be show good workspace feasibility and close to 0 would imply singularity.

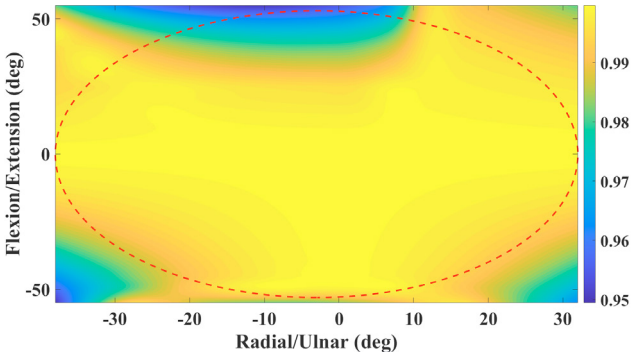

Fig. 6. Map of eigenvalue norm ratio calculated over the circumduction, with the dotted line representing approximate wrist circumduction

4.2 Visualization and Results:

Multibody modeling of the system is required for accurate simulation analysis. Multibody MATLAB toolbox, ANDY (Wang et al. (2018)), was used to model the Kinematics of the system. The wrist kinematics is modeled with first RUD then FE rotation sequence. Figure 5 illustrates the 3D representation of the reachable space of PEWTS equipped wrist. The reachability is illustrated for a point approximately near the knuckles of the middle finger. The blue and red lines represent the two exoskeleton linkages.

Figure 6 depicts the map of the eigenvalue norm ratio (24) over the range of wrist angles. The red dotted line approximately represents the circumduction of PEWTS equipped wrist. Figure 6 shows that over the circumduction the values of the norm ratio are close to 1, exhibiting good feasibility. This can be attributed to a parallel system setup. Since this setup requires excitation from both actuators to cover the circumduction at all times, this offers better controllability.

Figure 7 shows the map of relative excitation provided by actuators. This illustrates that the excitation increases with the Flexion motion and vice-versa for Extension for both the Exoskeleton subsystems. Similarly, excitation increases for Exoskeleton 1 (Figure 7 (a)) during Ulnar motion while it increases for Exoskeleton 2 (Figure 7 (b)) in Radial motion (Figure 2). Thus concurring with the design movements from figure 3.

5. CONCLUSION AND FUTURE WORK

This paper presents the design of PEWTS, a Parallel Exoskeleton for Wrist Tremor Suppression, designed to alleviate tremors in flexion/extension (FE) and radial/ulnar deviation (RUD) motions of the wrist. The proposed design uses linear Series Elastic Actuators to allow compactness and back-drivability, which offers better human compatibility. Theoretical analysis of PEWTS was presented with detailed Kinematic properties and a fundamental Dynamical model. The feasibility of PEWTS was investigated with the formulation of a multibody model and workspace analysis.

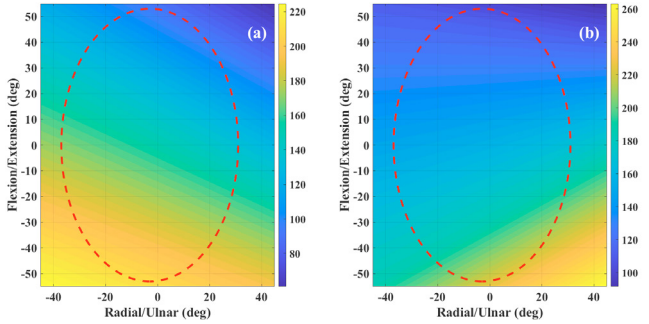

Fig. 7. Map of Input excitation (mm) provided by (a) Exoskeleton 1 and (b) Exoskeleton 2 over the circumduction

Further study is required to develop a more practical design that could be manufactured and be human-compatible and to evaluate the experimental validation. Further tuning of design parameters is required to allow larger circumduction. Validation of the dynamical model of the exoskeleton is essential for the implementation of required controls in future studies. Further research is required to build a suitable linear Series Elastic Actuator that would prove to be efficacious for this application.

6. ACKNOWLEDGEMENT

We would like to thank Dr. Jiamin Wang for their invaluable assistance in this research project. Their expertise, guidance, and willingness to share their time have been instrumental in shaping the direction of our work.

REFERENCES

Benito-Leon, J. and Louis, E.D. (2006). Essential tremor: Emerging views of a common disorder. *Nat. Rev. Neurol.*, 2(12), 666–678.

Diebel, J. (2006). Representing attitude: Euler angles, unit quaternions, and rotation vectors.

Fromme, N.P., Camenzind, M., Riener, R., and Rossi, R.M. (2019). Need for mechanically and ergonomically enhanced tremor-suppression orthoses for the upper limb: a systematic review. *J NeuroEngineering Rehabil*, 16(1), 93.

Heo, J., Jeon, H., Choi, E., Kwon, D., and Eom, G. (2018). Continuous sensory electrical stimulation for the suppression of parkinsonian rest tremor. *J Mech Med Biol*, 18(7), w1840006.

Jankovic, J. (2008). Parkinson's disease: Clinical features and diagnosis. *J. Neurol., Neurosurg. Psychiatry*, 79(4), 368–376.

Javidan, J, E., and A., P. (1992). Attenuation of pathological tremors by functional electrical stimulation ii: clinical evaluation. *Ann Biomed Eng.*, 20(2), 225–36.

Jeffrey and Binit (2014). Tremor. *JAMA Network*, 311(9), 948–954.

Kaelin-Lang, A., Gnädinger, M., and Mellinghoff, H.U. (2011). Parkinson's disease and the bones. *Swiss Med Wkly*, 141.

Kalia, L.V. and Lang, A.E. (2015). Parkinson's disease. *The Lancet*, 386(9996), 896–912.

Knabe, C., Lee, B., Orekhov, V., and Hong, D. (2014). Design of a compact, lightweight, electromechanical linear series elastic actuator. *IDETC-CIE*, Volume 5B: 38th Mechanisms and Robotics Conference.

Li, Z.M., Kuxhaus, L., Fisk, J., and Christophel, T. (2005). Coupling between wrist flexion–extension and radial–ulnar deviation. *Clinical Biomechanics*, 20(2), 177–183.

Louis, E. (2001). Essential tremor. *The New Engl. J. Med.*, 345(12), 887–891.

Lyons, K.E. and Pahwa, R. (2004). Deep brain stimulation and essential tremor. *Journal of Clinical Neurophysiology*, 21(1).

Maneski, L.P., Jorgovanovic´, N., Ilic´, V., Dos˘en, S., Keller, T., Popovic´, M.B., and Popovic, D.B. (2011). Electrical stimulation for the suppression of pathological tremor. *Med Biol Eng Comput*, 49, 1187–1193.

Moore, D.C., Crisco, J.J., Trafton, T.G., and Leventhal, E.L. (2007a). A digital database of wrist bone anatomy and carpal kinematics. *J Biomech*, 40(11), 2537–2542.

Moore, D.C., Crisco, J.J., Trafton, T.G., and Leventhal, E.L. (2007b). A digital database of wrist bone anatomy and carpal kinematics. *Journal of Biomechanics*, 40(11), 2537–2542.

Pascual-Valdunciel, A., Hoo, G.W., Avrillon, S., Barroso, F.O., Goldman, J.G., Hernandez-Pavon, J.C., and Pons, J.L. (2021). Peripheral electrical stimulation to reduce pathological tremor: a review. *J NeuroEngineering Rehabil*, 18(33).

Pons, J.L. (2008). *Wearable Robots: Biomechatronic Exoskeletons*. Wiley, England.

Rocon, E., Belda-Lois, J.M., Ruiz, A.F., Manto, M., Moreno, J.C., and Pons, J.L. (2020). Design and validation of a rehabilitation robotic exoskeleton for tremor assessment and suppression. *IEEE Trans. Neural Syst. Rehabil. Eng.*, 15(3), 367–378.

Sensinger, J.W. and Ff. Weir, R.F. (2006). Improvements to series elastic actuators. *IEEE/ASME International Conference on Mechatronics and Embedded Systems and Applications*, 1–7.

Taheri, B. (2013). *Real-Time Pathological Tremor Identification and Suppression in Human Arm Via Active Orthotic Devices*. Ph.D. thesis, Southern Methodist University, Dallas, TX.

Wang, J. (2022). *Design and Control of an Ergonomic Wearable Full-Wrist Exoskeleton for Pathological Tremor Alleviation*. Ph.D. thesis, Virginia polytechnic institute and state university, Blacksburg, VA.

Wang, J., Gupta, S.K., and Barry, O.R. (2020). Modeling analysis of the wrist dynamics via an ellipsoidal joint. *ASME paper. No. DSCC2020-3127*.

Wang, J., Kamidi, V.R., and Ben-Tzvi, P. (2018). A multibody toolbox for hybrid dynamic system modeling based on nonholonomic symbolic formalism. *Proceedings of the ASME, DSCC*, Volume 3: Modeling and Validation.